Dalton Transactions

RSC Publishing

PAPER

A novel tripodal tris-hydroxypyrimidinone sequestering agent for trivalent *hard* metal ions: synthesis, complexation and *in vivo* studies†

Cite this: *Dalton Trans.*, 2013, **42**, 6033

Sílvia Chaves,[a] Anabela Capelo,[b] Laurinda Areias,[b] Sérgio M. Marques,[a] Lurdes Gano,[c] M. Alexandra Esteves[b] and M. Amélia Santos*[a]

Received 5th October 2012,
Accepted 15th November 2012

DOI: 10.1039/c2dt32361c

www.rsc.org/dalton

A new tripodal hexadentate ligand, NTP(PrHPM)$_3$, having three hydroxypyrimidinone (HPM) chelating units attached to a nitrilotripropionic acid (NTP) has been prepared and studied in terms of thermodynamic stability of the complexes with iron, aluminium and gallium and it has been subsequently *in vivo* assayed for its capacity to remove *hard* metal ions from an animal model overloaded with ^{67}Ga. The anchoring of the HPM units to the NTP scaffold revealed to be an interesting alternative to the reported hexadentate tris(3-hydroxy-4-pyridinone) analogue, NTP(PrHP)$_3$, because the new tris-HPM ligand still keeps high chelating capacity for hard metal ions and presents better water-solubility (log P = −1.51). The *in vivo* studies show that NTP(PrHPM)$_3$ induces a faster clearance from main organs and an enhancement of overall excretion, as compared with the commercial drug, DFP, or the bidentate HPM compound (HOPY-PrN), albeit slightly lower than the tris-hydroxypyridinone analogue, NTP(PrHP)$_3$. The solution and *in vivo* results herein presented encourage further studies envisaging the potential clinical applications of hexadentate HPM derivatives as metal sequestering agents.

Introduction

Despite the biological importance of iron for all living cell, when in excess, it may become very toxic to the human body. In fact, humans have very little capacity for excretion of excess iron, which can result from its administration, as in beta-thalassemia patients, or from excess absorption, as in hemochromatosis.[1,2] Also, the nonessential ubiquitous aluminum (Al^{3+}), through different processes of exposure, can accumulate in specific organs leading to serious problems of toxicity,[3,4] namely bone disorders (vitamin-D-resistant osteomalacia) and neurological diseases, such as dialysis encephalopathy syndrome, and eventually Alzheimer's disease (AD).[5,6]

The therapeutic strategies to minimize the adverse effects of metal overload and misplaced related illnesses have led to the development of new chelating agents, which, by far, has been more focused on iron(III) than any other *hard* metal ions.[7] However, the physicochemical analogies between Fe^{3+} and other Lewis acid metal ions (*e.g.* Al^{3+}, Ga^{3+}) have orientated the potential use of many iron-chelators as Al-sequestering drugs or as radionuclide Ga-chelates for diagnostic drug.[8,9]

The main Al-binding protein in plasma is transferrin (Tf) which is only 30% saturated with Fe in normal serum, thus still keeping significant chelating capacity for other trivalent metal ions, such as Al.[10] Thus, in principle, Fe/Al-chelators must be able to compete with transferrin for those metal ions.

The first iron-chelating drug (since *ca.* 5 decades ago) for beta-thalassemia patients was the hexadentate tris-hydroxamate Desferrioxamine or Desferal (DFO).[11] However, its high water-lability and oral inactivity led to the disclosure of other orally active chelators, namely the bidentate 3-hydroxy-4-pyridinone (3,4-HP) Deferriprone (DFP) (in 1982)[12] and the tridentate Deferasirox or Exjade (ICL670), (approved by FDA in 2005),[13] although both also with recognized drawbacks. Concerning the aluminum chelators, DFO was also the first chelator introduced in clinical therapy, namely for treatment of osteomalacia and encephalopathy associated with severe dialysis Al-intoxication,[14] but its drawbacks led likewise to the search for alternatives.[8]

The need of stronger and orally active chelators for the decorporation of iron or other specific toxic *hard* metal ions such as aluminum or actinides has been worldwide recognized, and so, along the last 2 decades, we have assisted to an

[a]*Centro de Química Estrutural, Instituto Superior Técnico, Universidade Técnica de Lisboa, Av. Rovisco Pais 1, 1049-001 Lisboa, Portugal. E-mail: masantos@ist.utl.pt; Fax: +351-21-8464455; Tel: +351-21-8419273*

[b]*LNEG, Unidade de Pilhas de Combustível e Hidrogénio, Estr. Paço do Lumiar, 1649-038 Lisboa, Portugal*

[c]*IST/ITN, Instituto Superior Técnico, Universidade Técnica de Lisboa, Estrada Nacional No 10, 2686-953 Sacavém, Portugal*

†Electronic supplementary information (ESI) available. See DOI: 10.1039/c2dt32361c

intensive search for new metal sequestering agents, namely hydroxypyridinone(HP)-based compounds with mono- or polychelating capacity,[9,15,16] in view of single or combined drug administration protocols.[17]

As a step forward on the discovery of new strong iron chelators, we have decided to explore new ligands with hexadentate capacity, to guarantee the metal-full coordination, absence of ligand dilution effects and so iron-scavenging capacity at very low concentration. Thus, by paralleling a design strategy recently used in our group for tripodal hexadentate ligands,[18] we have substituted the chelating units, 3,4-HP by hydroxypyrimidinones (HPM), a kind of heterocyclic hydroxamate analogue with high hydrolytic stability, adequate hydrophilicity and chelating capacity, lying between those of the hydroxamic acids and the hydroxypyridinones.[19]

In particular, we describe herein the study of a novel tripodal tris-chelator, NTP(PrHPM)$_3$, having three HPM units appended to nitrilotripropionic acid as the anchoring skeleton (Scheme 1). After the synthetic methodology, we present the results of assessing its capacity for complexation with Fe^{3+}, Al^{3+} and Ga^{3+} in water, as well as the molecular modeling calculations (DFT) on the iron-complex to get some insight into its structure. The results from the study of the capacity of this new chelator for metal mobilization in mice pre-administrated with a radiotracer (^{67}Ga), as an animal model of metal-overload, are also analyzed. The discussion of all set of results is made in comparison with the reported properties for other synthetic chelators and bioligands.

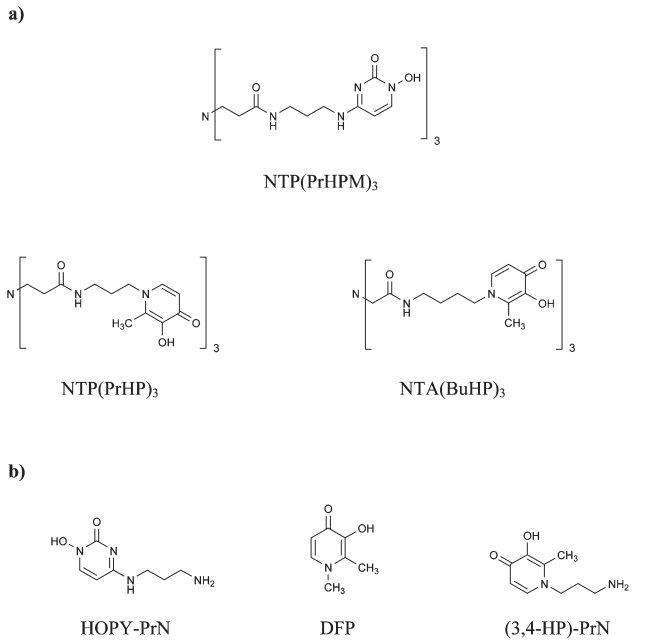

Scheme 1 Structural formulae for (a) tris-HPM and tris-HP hexadentate compounds and (b) HPM and HP bidentate compounds.

Results and discussion

Synthesis of the ligand, NTP(PrHPM)$_3$

The hexadentate compound (NTP(PrHPM)$_3$) was obtained through the attachment of three amino-bearing *O*-benzyl-hydroxypyrimidinone units (*O*-benzyl HOPY-PrN) to the tris-carboxylic scaffold (nitrilotripropionic acid, NTP) *via* the formation of amide linkages and final *O*-benzyl deprotection through standard methodologies, as described below.

The general procedure for the synthesis of NTP(PrHPM)$_3$ (3,3′,3″-nitrilotris(*N*-(3-(1-hydroxy-2-oxo-1,2-dihydropyrimidin-4-ylamino)propyl)propanamide)) is outlined in Scheme 2.

In the first step, 1-(benzyloxy)-4-(1′,2′,4′-triazol-1′-yl)-2-(1*H*)-pyrimidinone[19] **1** was reacted with 3-((*tert*-butoxycarbonyl)-amino)propylamine[20] to give 4-[3-((*tert*-butoxycarbonyl)amino)-propylamino]-1-(benzyloxy)-2(1*H*)-pyrimidinone **2** in 74% yield. Removal of the Boc group involved treatment with HCl in 1,4-dioxane[21] and provided 4-(3-aminopropylamino)-1-(benzyloxy)-2(1*H*)-pyrimidinone hydrochloride **3** in quantitative yield. The coupling of this amine-bearing HPM side arm to the backbone 3,3′,3″-nitrilotripropanoic acid (NTP) involved a pre-activation of this tris-carboxylic acid with TBTU, under anhydrous conditions, followed by addition of compound **3**, after its neutralization with *N*-methylmorpholine (NMM), affording the pre-final product **4** (37% yield). The final ligand (NTP(PrHPM)$_3$) was obtained in almost quantitative yield (91%), by *O*-benzyl deprotection using a standard hydrogenolysis with 10% Pd/C as a catalyst.

Solution equilibrium studies

The physico-chemical characterization of the tris-HPM ligand, NTP(PrHPM)$_3$, was carried out in aqueous solution, namely the study of the acid–base properties and the lipo-hydrophilic character, as well as its complexation ability towards *hard* metal ions (Fe^{3+}, Ga^{3+} and Al^{3+}). Discussion of the results is made on the basis of comparison with previously reported tripodal hexadentate tris-HP compounds (NTP(PrHP)$_3$ and NTA-(BuHP)$_3$)[19,22] and also with bidentate compounds, such as the HPM derivative (HOPY-PrN)[20] or the commercial drug DFP (see Scheme 1).

Acid–base behavior

The acid–base properties of NTP(PrHPM)$_3$ were mainly studied by fitting analysis of the potentiometric titration data, which provided the protonation constants; a ^{1}H NMR spectroscopic titration was used to check the protonation sequence; a UV spectrophotometric titration of the ligand was also performed to determine the spectral parameters of the various protonated species to be subsequently introduced in the equilibrium model of the Ga^{3+}/NTP(PrHPM)$_3$ system.

The compound was isolated in its neutral form (H_3L), whereas, when fully protonated, it has seven dissociable protons (H_7L^{4+}). The stepwise protonation constants, obtained from pH-potentiometric studies for NTP(PrHPM)$_3$, are summarized in Table 1, which also includes the corresponding reported values for some other HPM and HP analogues.

Analysis of calculated stepwise protonation constants (log K_i) for NTP(PrHPM)$_3$ evidences the existence of a first set

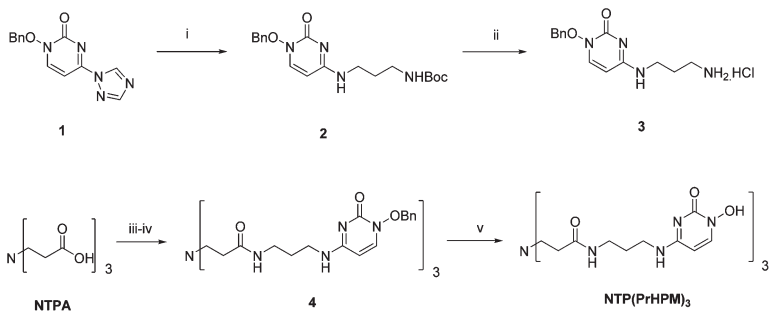

Scheme 2 *Reagents and conditions*: (i) $H_2N(CH_2)_3NHBoc$, dry THF, reflux, 16 h; (ii) 4 M HCl in 1,4-dioxane, 0 °C, 4 h; (iii) TBTU, NMM, dry DMF, r.t., 1 h; (iv) **3**, NMM, dry DMF, r.t., 6 h; (v) H_2, Pd/C, MeOH, 2 h, r.t.

Table 1 Stepwise protonation constants (log K_i) and partition coefficient (log P) of $NTP(PrHPM)_3$, as well as global formation constants of the M^{3+} complexes. Data for other tripodal compounds, HOPY-PrN and DFP are also presented for comparison (T = 25.0 ± 0.1 °C, I = 0.1 M KCl)

Ligand	log K_i	$M_mH_hL_l$ (m,h,l)	log β ($Fe_mH_hL_l$)	log β ($Ga_mH_hL_l$)	log β ($Al_mH_hL_l$)	log P
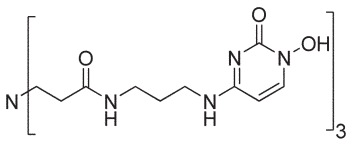	8.25(2)	(1,5,1)	38.93(4)	36.61(3)	—	−1.51
	7.22(3)	(1,3,1)	36.32(4)	34.20(6)	31.26(5)	
	6.78(2)	(1,1,1)	29.36(3)	28.12(7)	24.57(5)	
	6.02(3)	(1,0,1)	—	23.50(9)	17.81(8)	
	3.29(6)					
	2.61(9)					
	2.0(1)	**pM***	—	**23.3**	**17.7**	
$NTP(PrHPM)_3$						
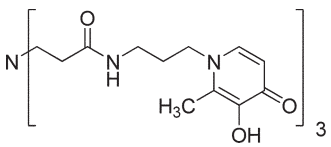	9.946(9)	(1,5,1)	47.62(5)	46.70(1)[b]	44.69(6)	−1.24
	9.84(1)	(1,3,1)	45.29(5)	44.00(4)[b]	40.01(5)	
	9.091(8)	(1,1,1)	40.56(3)	38.79(2)[b]	34.72(4)	
	6.77(1)	(1,0,1)	35.21(1)	33.34(3)[b]	28.13(3)	
	3.81(1)					
	3.14(1)					
	2.76(2)	**pM***	**29.4**	**27.5**[b]	**22.4**	
$NTP(PrHP)_3$[a]						
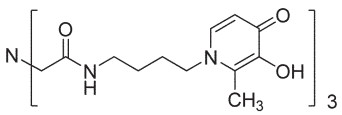	9.98(2)	(1,5,1)	42.30(2)[c]		—	−1.40
	9.83(3)	(1,4,1)	40.81(5)[c]	—	37.45(4)	
	8.94(4)	(1,2,1)	38.53(3)[c]	—	33.55(1)	
	3.88(4)	(1,0,1)	33.50(1)[c]		27.65(6)	
	3.11(5)					
	2.35(5)					
	1.4(1)	**pM***	**27.9**[d]		**22.0**	
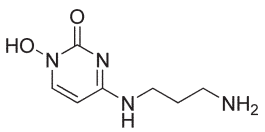	10.11(2)[e]	(111)	19.88(4)[e]	18.74(6)	16.84(2)[e]	−1.43
	6.84(4)[e]	(122)	38.12(6)[e]	36.11(4)	34.04(4)[e]	
	2.21(5)[e]	(133)	55.26(5)[e]	52.42(3)	49.67(2)[e]	
		(123)	48.04(3)[e]	45.63(4)	**13.1**	
		pM*	**16.1**	**14.9**		
HOPY-PrN						
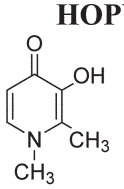	9.77	**pM***	**19.3**[f]	**19.2**[g]	**16.0**[f]	−0.85
	3.62					−1.03[h]
DFP[f]						

*pM values at pH = 7.4 ($C_M = 10^{-6}$ M, $C_L/C_M = 10$). [a] Ref. 18. [b] Ref. 22. [c] Values determined in 3% DMSO. [d] Admitting that there is no precipitation under the concentration conditions of pM determination. [e] Ref. 19. [f] Ref. 23. [g] Ref. 24. [h] Ref. 25.

of four values in the range 6.0–8.2, corresponding to three hydroxyl groups of the HPM moieties plus the anchoring backbone amine group; the second set of values is in the range 2.0–3.3, being attributed to the 4-imine groups of the side chains. These results are in accordance with the protonation constants hitherto obtained for the hydroxyl (log K_2 = 6.84)

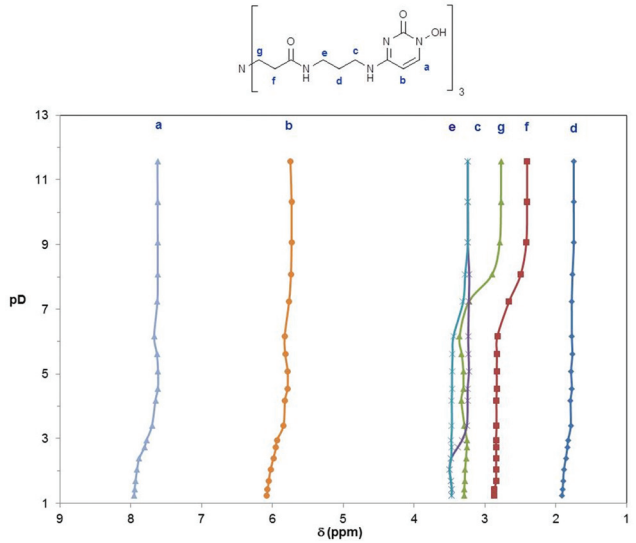

Fig. 1 ^{1}H NMR titration curves of NTP(PrHPM)$_3$ ($C_L = 5 \times 10^{-4}$ M).

and 4-imine (log K_3 = 2.21) groups of HOPY-PrN. The protonation constants calculated for the HPM hydroxyl groups are lower than those obtained for the corresponding HP analogues (9.1–9.9 for the tris-HP, 9.77 for DFP), which can be due to the electron withdrawing and resonance effects of the aromatic ring, as well as to the electron-withdrawing effect of a second ring-nitrogen, contributing to the stabilization of the negative charge of the conjugate base. Moreover, the very acidic character of the 4-imine groups, requiring the addition of acid excess to guarantee the ligand full protonation, must be due to the existence of enamine/imine equilibrium together with the above referred electron-withdrawing and resonance effects of the aromatic ring.

The set of ^{1}H NMR titration curves (Fig. 1) presents downfield shifts of the non-labile protons, namely in the ranges pD 6–9 (protons a, b, e, f, g) and pD 2–3.5 (protons a, b, c, d), which give some support to the attributed protonation sequence. The protonation of the hydroxyl and the backbone amine groups is practically simultaneous, as evidenced by a detailed analysis of these curve profiles, namely the occurrence of large downfield shifts on protons g and f (due to the nearby amine group) close to the pH range of hydroxyl group protonation (unfortunately, not clearly evidenced in this figure because the curve profiles for protons a and b are quite smooth).

Though the attribution of the four calculated macroconstants in the higher pH range to individualized protonation processes renders difficult, analysis of Fig. 1 seems to suggest that log K_3 may be mainly ascribed to the protonation of the backbone amine, taking into account the isotopic correction.[26] The value obtained for NTP(PrHPM)$_3$ (6.78) would be quite close to the corresponding value for NTP(PrHP)$_3$ (6.77), thus indicating that for these tripodal ligands, sharing the same backbone, the protonation of the apical amine is quite independent of the appended chelating arms.

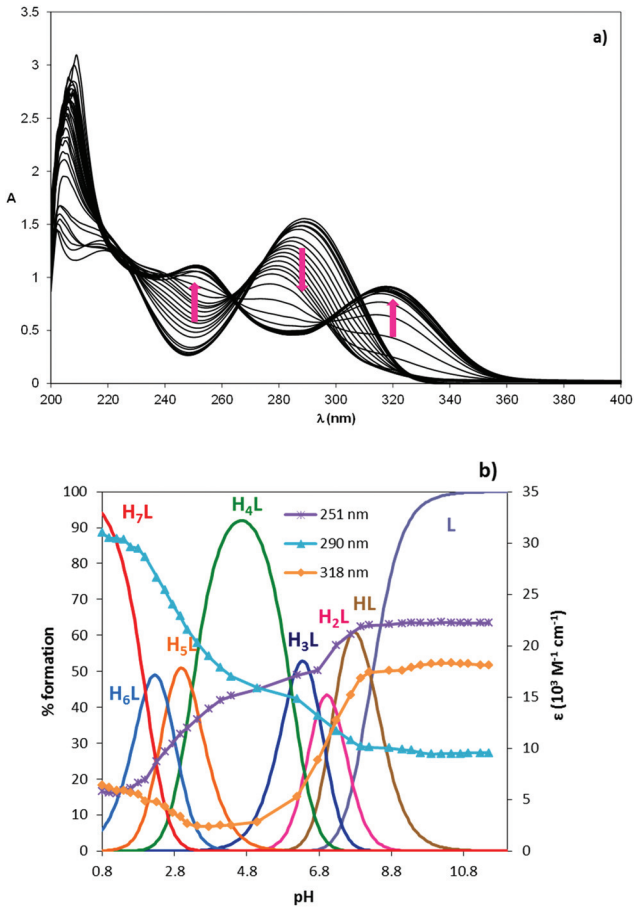

Fig. 2 (a) Electronic spectra (pH 0.8–11.5) and (b) species distribution curves with molar extinction coefficients at maximum absorption wavelengths for NTP(PrHPM)$_3$ ($C_L = 5 \times 10^{-5}$ M).

Though the acid–base properties of NTP(PrHPM)$_3$ were mainly assessed by potentiometry and ^{1}H NMR (see above), we have also included herein the spectrophotometric titration of this ligand (see Fig. 2a), a requirement for the subsequent UV spectrophotometric study of the gallium complex formation (see below), as well as a combination of spectral data with the species distribution curves (Fig. 2b).

Analysis of Fig. 2b evidences that in the range 3.2 < pH < 6, the major protonated species is H_4L^+; at the physiological pH, H_3L (8%), H_2L^- (33%), HL^{2-} (51%) and L^{3-} (7%) coexist, while for pH above 8.3 the ligand is essentially deprotonated (L^{3-}). This figure also shows that the species H_5L^{2+}, H_4L^+, H_3L, H_2L^- and HL^{2-} absorb at 251 nm, while H_7L^{4+} absorbs at 290 nm; the absorptivity values at 318 nm reveal that the main species absorbing at this wavelength are HL^{2-} and L^{3-}. Therefore, 290 nm and 318 nm seem to correspond to the absorption maximum wavelengths for the chromophores of the completely protonated (H_7L^{4+}) and deprotonated forms (HL^{2-} and L^{3-}) of the hydroxypyrimidinone, respectively. At 251 nm, it is evidenced an equilibrium between species with different partially protonated hydroxyl/imine moieties present.

An identical spectrophotometric study was also performed for the ligand HOPY-PrN, spectra of which presented absorption maximum at 251, 285 and 318 nm (Fig. S1†).

Lipo-hydrophilic character

The lipo-hydrophilic character of NTP(PrHPM)$_3$ and HOPY-PrN was assessed *via* the corresponding partition coefficients (log *P*) between 1-octanol and a TRIS-buffered aqueous solution at the physiological pH. The value obtained for NTP(PrHPM)$_3$ (−1.51) is quite close to others previously reported for analogous compounds, namely hexadentate HP derivatives with similar anchoring groups.[19] This value is slightly higher than those obtained for NTP(PrHP)$_3$ (−1.24) or NTA(BuHP)$_3$ (−1.40), which seems according to the higher water solubility of HPM as compared with HP derivatives. This difference is also supported by the fact that, at pH 7.4, NTP(PrHPM)$_3$ is mostly negatively charged (*ca.* 91%, as H_2L^-, HL^{2-} and L^{3-}) while NTP (PrHP)$_3$ is predominantly in the neutral form (80% H_3L) and only 20% as a monoprotonated species (H_4L^+).

The HOPY-PrN compound is also slightly more hydrophilic (log *P* = −1.43) than the HP bidentate analogues, such as the drug DFP (log *P* = −0.85) or 3,4-HP-PrN (log *P* = −1.25). These differences can be partially rationalized on the basis of distribution curves. At pH 7.4, HOPY-PrN presents as 22% monoprotonated species (H_2L^+), while DFP as a 100% neutral form (HL) and 3,4-HP-PrN as 98% H_2L^+ species. Of course, besides the species charge, other factors are also determinant for the lipo-hydrophilic character, namely the solute–solvent interaction. In fact, at pH 7.4, DFP is in the neutral form but presents some hydrophilic character.

Metal chelating capacity

The complexation ability of NTP(PrHPM)$_3$ towards Fe^{3+}, Ga^{3+} and Al^{3+} was studied in solution by determination of the global stability constants of the complexes which allowed the assessment of species distribution under different pH conditions. Those studies involved potentiometric and UV/Vis spectrophotometric titrations with subsequent fitting analysis of the experimental data with HYPERQUAD 2008[27] and PSEQUAD[28] programs.

The iron complexation was studied by UV/Vis spectrophotometry because at pH = 2 two protonated complex species (FeH_5L and FeH_3L) were already formed, thus precluding the use of potentiometry. This study was performed in two stages: for pH ≤ 2, a batch titration was used, in which calculated amounts of HCl and KCl were added in order to obtain the desired pH value and to keep constant the ionic strength; for pH > 2, a standard automatic titration was carried out. The first titration stage allowed the determination of the stability constants corresponding to the species FeH_5L and FeH_3L; these values were kept constant and introduced in the equilibrium model for pH > 2, which allowed the calculation of β_{FeHL}. The determination of β_{FeL} became impossible, since under our experimental conditions, precipitation occurred above pH 6.5, probably due to the formation of the neutral FeL species or even mixed hydroxo-ligand complexes. Analysis of

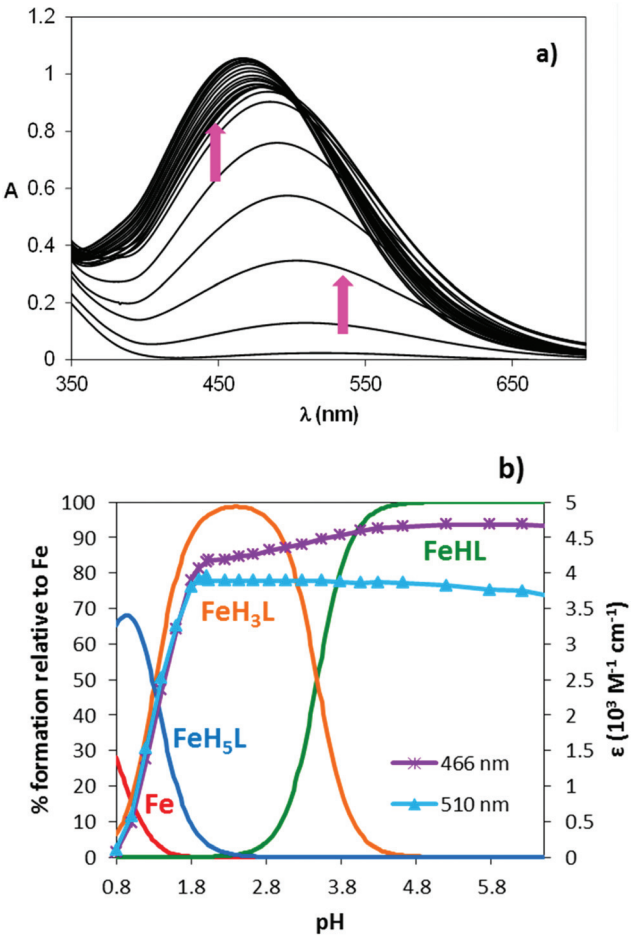

Fig. 3 (a) Electronic spectra (pH 0.8–6.5) and (b) species distribution curves with molar extinction coefficients at maximum absorption wavelengths for the Fe^{3+}/NTP(PrHPM)$_3$ system (C_L/C_{Fe} = 1.2, C_L = 2.7 × 10^{-4} M).

the UV-Vis absorption spectra registered at different pH values for the Fe^{3+}/NTP(PrHPM)$_3$ system in Fig. 3a shows one isosbestic point at *ca.* 500 nm, corresponding to the interconversion of the tetrachelate complex (FeH_3L) to the hexachelate complex (FeHL). The species distribution curves associated with the proposed equilibrium model for the Fe^{3+}/NTP(PrHPM)$_3$ system combined with the absorptivity at two wavelengths (466 and 510 nm) (Fig. 3b) show that the maximum absorption at 466 nm (4659 M^{-1} cm^{-1}) corresponds to the ligand to metal charge-transfer (CT) band of the trischelate (FeHL) complex, while the band at 510 nm (3801 M^{-1} cm^{-1}) corresponds to the CT band of the bischelate (FeH_3L) complex. The spectral parameters obtained for the trischelate are quite close to the reported values for the CT bands of ferric trischelated complexes with hydroxypyrimidinone analogues such as the hexadentate 3HOPY$_5$ (465 nm, 4550 M^{-1} cm^{-1})[29] or the bidentate HOPY-PrN (465 nm, 5624 M^{-1} cm^{-1}).[19] Thus, these studies evidenced the high iron chelating capacity of this ligand, since the trischelate (FeHL) species, formed through the {*O*,*O*} chelation of the adjacent *N*-hydroxo and keto-oxygen groups of the three *arms*, is predominant at pH above 3.5.

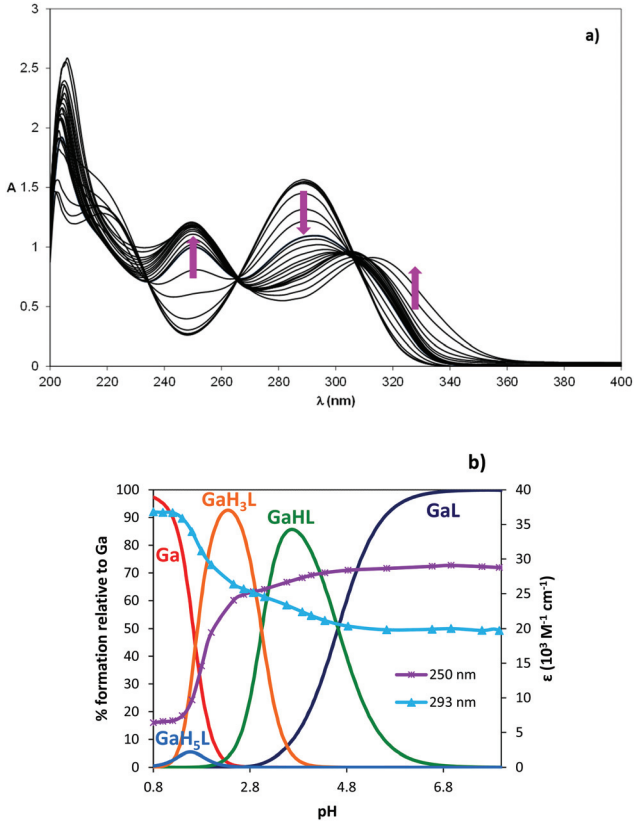

Fig. 4 (a) Electronic spectra (pH 0.8–8.9) and (b) species distribution curves with molar extinction coefficients at maximum absorption wavelengths for the Ga^{3+}/NTP(PrHPM)$_3$ system (C_L/C_{Ga} = 1.2, C_L = 5 × 10^{-5} M).

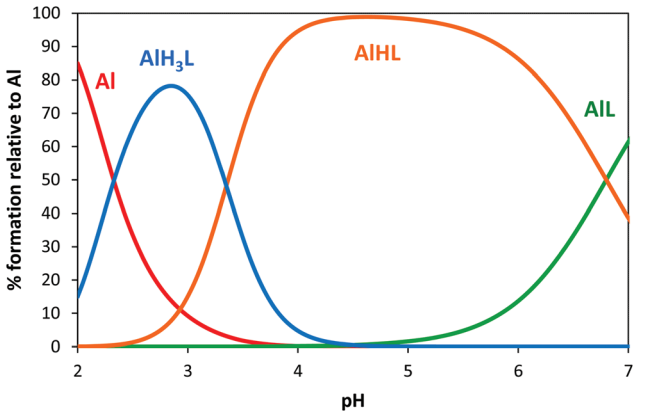

Fig. 5 Species distribution curves for the (1 : 1) Al^{3+}/NTP(PrHPM)$_3$ system (C_L = 4 × 10^{-4} M).

Table 2 pM* (M = Fe, Ga, Al) values at the physiological pH for NTP(PrHPM)$_3$ and some selected ligands.

Ligand	pFe	pGa	pAl
NTP(PrHPM)$_3$	—	23.3	17.7
NTP(PrHP)$_3$	29.4[a]	27.5[b]	22.4[a]
NTA(BuHP)$_3$ [a]	27.9[c]	—	22.0
IDA(HP)$_2$ [d]	25.8	22.9	18.8
EDTA(HP)$_2$ [e]	26.3	24.9	19.0
EDTA[f]	23.4	20.2	16.2
DTPA[f]	24.6	20.9	15.7
DOTA[f]	24.3	18.8	13.2
DFO	26.5[g]	22.4[h]	19.3[h]
DFP	19.3[i]	19.2[j]	16.0[i]
Transferrin	20.3[k]	20.3[l]	14.5[m]

*C_M = 10^{-6} M, C_L/C_M = 10 (pH = 7.4). [a] Ref. 18. [b] Ref. 22. [c] Admitting that there is no precipitation for the low concentration values of pM determination. [d] Ref. 30. [e] Ref. 31. [f] Ref. 32. [g] Ref. 33. [h] Ref. 34. [i] Ref. 23. [j] Ref. 24. [k] Ref. 33. [l] Ref. 35. [m] Ref. 10.

Regarding the Ga^{3+}/NTP(PrHPM)$_3$ system, since the gallium-complex formation also started below pH 2, we have also performed a two-stage spectrophotometric titration under 1 : 1 metal–ligand stoichiometry, using the same methodology cited above for the iron complexation (Fig. 4a). The batch titration (pH ≤ 2) allowed the determination of the global stability constants and spectral data of the species GaH_5L and GaH_3L, while the second stage titration (pH > 2) enabled the determination of β_{GaHL} and β_{GaL}. Analysis of the speciation diagram for this system (Fig. 4b) discloses the presence of the bischelate GaH_3L as a major species for pH between 1.7 and 3 and above pH 3 the predominance of the trischelate as a monoprotonated (GaHL) or a non-protonated (GaL) species. Fig. 4b shows also that the fully protonated complex (GaH_5L) absorbs at 293 nm, while the absorbance at 250 nm is mostly due to the hexacoordinated gallium complexes (GaHL and GaL).

The 1 : 3 Ga^{3+}/HOPY-PrN system was studied by potentiometry, keeping constant the value of β_{GaHL} previously determined by spectrophotometric titration under 1 : 1 M–L stoichiometric conditions, and the obtained Ga^{3+} complexation model is presented in Table 1.

The study of Al^{3+} complexation was performed by potentiometry using a 1 : 1 metal-to-ligand stoichiometric ratio (Fig. S2†). The Al^{3+}/NTP(PrHPM)$_3$ titration curve shows an inflexion at a = 2 (a is the ratio between the number of millimoles of a base and that of a ligand), which means that, as expected, the backbone amine is not involved in the metal coordination. Moreover, analysis of that titration curve also suggests that the deprotonation of that amine group may be followed by the formation of hydroxo species above pH 7. Nevertheless, once more the high chelating capacity of this ligand for Al^{3+} seems evidenced in Fig. 5, since the distribution curves show that the main forms of the aluminium complex above pH *ca*. 3.3 are tris-chelated species.

Comparison of the metal chelating capacity of ligands with different acid–base behaviour and denticity is usually made on the basis of the pM parameter (pM = −log[M^{n+}], C_L/C_M = 10, C_L = 10^{-5} M at pH = 7.4). Unfortunately, the pFe value could not be calculated herein due to solubility limitations above pH 6.5, under our experimental conditions. This rendered impossible the determination of β_{FeL} which would result in a calculated pFe value at pH 7.4 with no real meaning. In order to try to make an adequate comparison of the iron chelating ability of this ligand with that of other ligands contained in Table 2, the pFe value was determined at pH 6.0. It was found that NTP(PrHPM)$_3$ (pFe 19.7) is a stronger iron chelator than the drug

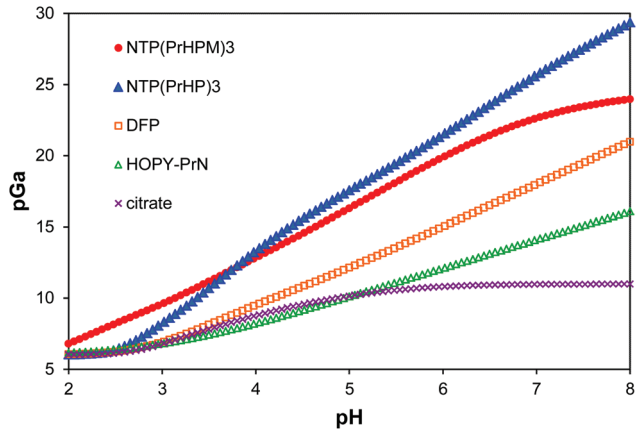

Fig. 6 Metal complexation strength, reported as pGa *versus* pH, for some selected ligands.

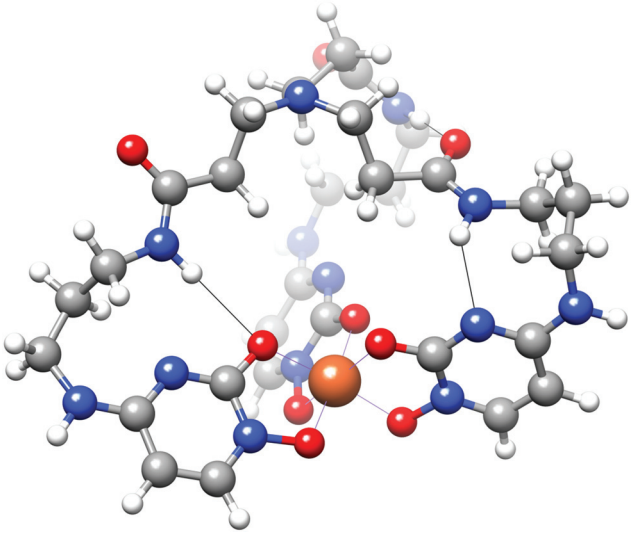

Fig. 7 DFT-minimized structure of the complex Fe^{3+}–NTP(PrHPM)$_3$. The O–Fe metal coordination bonds are represented as purple lines and H-bonds as black lines. C atoms are grey, H atoms white, N atoms blue, O atoms red and Fe atom orange.

DFP (pFe 15.4), although it is weaker for iron than the hexadentate tris-HP (pFe 23.7–24.5), the tetradentate bis-HP (pFe 21.6–22.5) or the commercial chelators EDTA, DTPA and DOTA. Concerning the pGa and pAl values determined for NTP(PrHPM)$_3$, they are considerably high, albeit lower than those for the hexadentate HP analogues (NTP(PrHP)$_3$ and NTA(BuHP)$_3$). This is according to the reported trend of the bidentate HPM derivatives which usually present lower pM values than HP analogues (*e.g.* HOPY-PrN and DFP)[16] (see Fig. 6).

Moreover, Table 2 shows that NTP(PrHPM)$_3$ presents pM values in the range of the previously calculated values for bis-HP compounds (IDA(HP)$_2$ and EDTA(HP)$_2$), but evidencing higher affinity than other currently used drugs for Al decorporation (DFP, EDTA, DTPA, DOTA) or even for diagnostic probe containing ^{68}Ga (DFP, DFO, EDTA, DTPA, DOTA).

Table 2 also suggests that NTP(PrHPM)$_3$ is able to compete, from the thermodynamic point of view, with transferrin for the complexation with those hard metal ions. Of course that this is a somehow limited view of the problem, since computational models predicted already significant time-dependent non-equilibrium binding of Al by ligands in competition with transferrin,[36] which undoubtedly demonstrates the importance of both kinetic and thermodynamic control for metal distribution in biological systems.

In general, it can be concluded that NTP(PrHPM)$_3$ is a better chelator for the *hard* metal ions studied than the drug DFP, being also more efficient for gallium and aluminium complexation than several currently used chelators, such as EDTA, DTPA or DOTA.

Molecular modeling of the Fe^{3+} complex

It is widely accepted that one of the best techniques to disclose the lowest energy structure of a molecule is by X-ray diffraction of single crystal. Unfortunately, until now all our efforts to obtain good crystals and get the 3D conformation of the ferric complex with NTP(PrHPM)$_3$ revealed unfruitful. Hence, we have decided to use molecular simulations based on Density Functional Theory (DFT) to get the optimized structure for the Fe^{3+}–NTP(PrHPM)$_3$ complex.

The DFT modeling studies were carried out using Gaussian 03W software[37] in two steps with the B3LYP hybrid functional. The first step was aimed mainly at optimizing the geometry of the ligand, while the second one, involving a more complex basis set (LANL2DZ), was more appropriate to treat the Fe atom. In order to perform the structural optimization of the Fe^{3+}–NTP(PrHPM)$_3$ complex, two structures were designed. The first one, in a so-called "in" conformation, displays the central N atom with its free orbital pointing inwards the complex structure, and the second one, with an "out" conformation, has the N atom pointing outwards. The two calculation processes converged and resulted in two different structures, which still maintained the original "in" and "out" conformations of the apical N atom. However, these two structures presented a difference in their global formation enthalpy of 0.0080008 Hartree (5.02 kcal mol^{-1}), the "out" conformation being the most stable (see the final structure in Fig. 7). Interestingly, from previous modeling (DFT calculations) of the corresponding Fe^{3+}–NTP(PrHP)$_3$ complex the "out" conformation also appeared as slightly more stable than the "in" conformation.[19] This structure is slightly twisted (see Fig. 7, the right and left arms are drawn out and flattened over the back arm), which necessarily results in some energy penalty from this symmetry break and structure strain. However, such energy loss must be largely compensated by the stabilization energy afforded with the formation of three H-bonds between the three amide NH groups with one N atom and one carbonyl O atom of the HPM rings (2.48 and 2.18 Å, respectively), and with a carbonyl O atom of one arm (1.91 Å; see Fig. 7, black solid lines). Regarding the metal ion coordination sphere, the optimized structure maintained, as expected, the original

input octahedral geometry with the ferric ion being chelated through the six HPM-O atoms of the ligand, and Fe–O bond lengths ranging between 1.92–1.97 Å. Concerning the final "in" geometry structure (not shown), this structure displayed an even more distorted and asymmetric geometry. It displayed two H-bonds between the NH atoms of two amide groups with one another and with one ring N atom, obviously not stabilizing enough to make it the lowest energy conformation of the Fe^{3+}–NTP(PrHPM)$_3$ complex.

In vivo assays

The ability of the new hexadentate chelating agent, NTP(PrHPM)$_3$, for *in vivo* mobilisation of ^{67}Ga was assessed in mice as an animal model of metal-overload pathologies, owing to the well-known similarities between Ga^{3+} and other *hard* metal ions associated with those diseases (*e.g.* Fe^{3+} and Al^{3+}). In spite of the fact that the suitability of Ga as a substitute for Al in biological systems seems to be controversial, since some authors agree[38] while others indicate different behaviours,[39,40] the ^{67}Ga radionuclide appears to be quite convenient for the bioassays and it is herein expected to give some clue about the *in vivo* efficacy of the ligand to mobilize those metals.

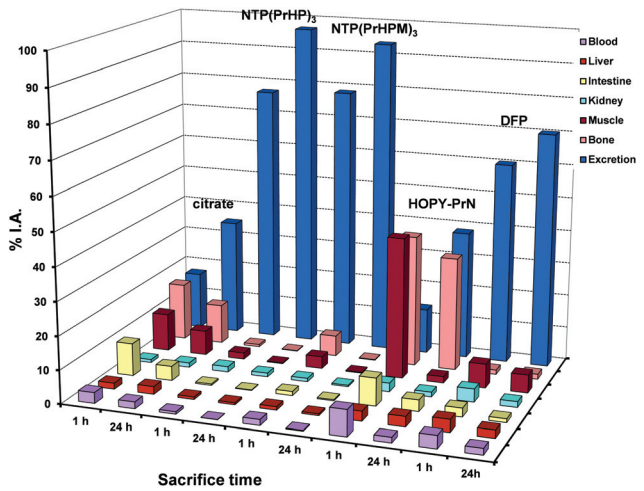

Fig. 8 Biodistribution data in the most relevant organs, expressed as % I.A./organ for ^{67}Ga-citrate (iv injection) and ^{67}Ga-citrate with simultaneous intraperitoneal injection of the ligands NTP(PrHP)$_3$, NTP(PrHPM)$_3$, HOPY-PrN and DFP, 1 and 24 h after intravenous administration in female mice (n = 3–5).

Biodistribution studies, at specific post-injection times, were carried out by i.v. administration of the radiotracer immediately followed by i.p. injection of the ligand solution, as previously reported by us.[23] The ^{67}Ga tissue distribution was compared to its pattern without simultaneous administration of any chelator (Fig. 8) and the most representative tissue distribution data are presented in Table 3.

Analysis of the biodistribution profiles clearly shows that the co-administration of the ligand NTP(PrHPM)$_3$ and the radiotracer interferes in the usual tissue distribution of the radioactive metal, inducing a faster clearance from main organs and highly enhancing the overall excretion rate of radioactivity from whole animal body. Furthermore, no significant uptake was found in any major organ, except those related with excretory routes. The high rate of excretion is a relevant sign of the good capacity of this hexadentate ligand for the *in vivo* Ga^{3+} chelation. Hence, this favourable *in vivo* behaviour points to the potential usefulness of this ligand as a decorporating agent of *hard* trivalent metal ions.

Comparison between the biodistribution data, due to the administration of the citrate radiotracer followed by injection of the ligand and due to the administration of the ^{67}Ga–NTP(PrHPM)$_3$ complex (previously prepared with high yield and radiochemical purity) in the same animal model, at 4 h after injection (data not shown) evidences a very good analogy, especially on the uptake and clearance from main organs as well as the excretion rate. Thus, these findings indicate a rapid kinetics of *in vivo* complex formation and high affinity of the ligand to the metal ion.

The effect of this ligand on the metal uptake and clearance from the main organs of our animal model is illustrated in the histogram of Fig. 8 (at 1 h and 24 h after administration), in comparison with the corresponding effect due to the similar administration of analogues (the hexadentate NTP(PrHP)$_3$ as well as the bidentates HOPY-PrN and the drug DFP).

Although the administration of both hydroxypyrimidinone-based compounds alters the metal biodistribution, the capacity for the ^{67}Ga removal from tissues is obviously higher for the hexadentate ligand NTP(PrHPM)$_3$ than the bidentate

Table 3 Biodistribution data in the most relevant organs, expressed as % I.A./organ for ^{67}Ga-citrate and ^{67}Ga-citrate with simultaneous intraperitoneal injection of the ligand NTP(PrHPM)$_3$ at 15 min, 1 h, 4 h and 24 h, after intravenous administration in female mice (n = 3–5).

	I.A./organ (%)						
	^{67}Ga-citrate			^{67}Ga-citrate + NTP(PrHPM)$_3$			
Organs	15 min	1 h	24 h	15 min	1 h	4 h	24 h
Blood	10.2 ± 2.3	3.2 ± 1.9	2.0 ± 0.8	8.5 ± 4.3	1.7 ± 0.2	0.5 ± 0.08	0.19 ± 0.05
Liver	2.7 ± 1.3	1.8 ± 0.2	2.3 ± 1.0	2.0 ± 0.8	1.0 ± 0.2	0.73 ± 0.04	0.5 ± 0.1
Intestine	4.0 ± 0.4	9.8 ± 1.6	4.3 ± 0.7	2.2 ± 0.4	1.3 ± 0.5	1.2 ± 0.1	0.3 ± 0.1
Kidney	1.5 ± 0.4	0.9 ± 0.1	1.3 ± 0.3	3.9 ± 0.8	1.0 ± 0.1	0.6 ± 0.1	0.39 ± 0.07
Muscle	20.2 ± 2.3	11.3 ± 3.7	7.4 ± 0.8	12.3 ± 3.3	3.6 ± 0.2	0.8 ± 0.2	0.15 ± 0.04
Bone	13.8 ± 3.5	17.1 ± 7.5	11.8 ± 3.1	10.8 ± 2.5	6.2 ± 0.5	4.8 ± 1.0	2.9 ± 0.7
Excretion	6.7 ± 2.9	17.2 ± 3.6	35.0 ± 7.2	28.7 ± 8.9	78.5 ± 2.2	90.9 ± 0.2	93.8 ± 1.4

analogue HOPY-PrN. In fact, the administration of HOPY-PrN led to slower clearance on blood and soft-tissue, but higher bone retention and no improvement in the overall radioactivity excretion, thus excluding its potential use for chelating therapy.

A comparative analysis of the ^{67}Ga mobilization induced by the hexadentate ligands shows that NTP(PrHPM)$_3$ led to slightly higher bone radioactivity accumulation than the 3,4-HP analogue. A further comparison between the biodistribution data obtained upon administration of the new ligand and of the chelating drug (DFP) evidences the ability of the new compound for a faster metal clearance from the main organs, especially from blood and muscle, as well as an enhancement of the overall metal excretion.

In summary, the high *in vivo* ability of NTP(PrHPM)$_3$ to complex with Ga, promoting its rapid clearance from main organs and fast overall excretion rate, anticipates its potential usefulness as a drug candidate for metal chelation therapy.

Conclusions

A new tripodal hexadentate hydroxypyrimidinone derivative – NTP(PrHPM)$_3$ – has been synthesized and studied in solution and *in vivo* in order to evaluate its capacity as a metal sequestering agent. The developed compound revealed high chelating capacity towards trivalent *hard* metal ions (Fe, Al, Ga), with pM values in the same order of magnitude of the tetradentate bis-HP compounds and higher values than those of the clinically used drug DFP. Concerning the capacity of *in vivo* metal mobilization, NTP(PrHPM)$_3$ presents a favorable biodistribution profile, a high *in vivo* chelating efficiency and a faster clearance from main organs, especially from blood and muscle, as well as an enhancement of overall excretion, when compared with the drug DFP. The herein collected data give support to the potential interest of this chelator in detoxification of *hard* metal ions.

Experimental

General information and instrumentation

The chemicals were of analytical reagent grade, being used without further purification. Whenever necessary, the organic solvents were dried according to standard methods.[41] Chemical reactions were followed by thin layer chromatography (TLC) on silica gel 60 F254 plates with 0.2 mm layer thickness from Macherey-Naguel and the compounds were visualized by illumination under UV light at 254 nm.

Melting points were determined in a Reichert Thermovar apparatus and are uncorrected. FTIR spectra were recorded on a Perkin-Elmer Spectrum BX v5.3.1 spectrometer. Fourier transform (FT) NMR spectra were run on a BRUKER AVANCE 400 MHz Ultra-Shield spectrometer at Faculty of Sciences of Lisbon University (compounds **2–3**) and at the Instituto Superior Técnico (compounds **4** and NTP(PrHPM)$_3$). The chemical shifts (δ) are reported in ppm from the internal references TMS (tetramethylsilane), for organic solvents, or DSS (3-trimethylsilyl-propionic acid-d4 sodium salt) for D_2O, and the coupling constants (J) in Hz. Whenever necessary, the peak attribution was aided by performing 2D correlation experiments (*e.g.* COSY, HSQC). Electron Spray Ionization (ESI) mass spectra (MS) were performed on an ESI-QIT/MS Bruker HCT (electrospray ionisation quadrupole ion trap mass spectrometer), operated in the positive mode. Microanalyses were performed on a Fisons EA1108 CHNF/O instrument.

In the complexation studies, the $FeCl_3$ (0.0177 M), $AlCl_3$ (0.0393 M) and $GaCl_3$ (4.16×10^{-3} M) solutions were standardized by atomic absorption (Fe and Al) and inductively coupled plasma emission (Ga). The metal solutions were prepared in acid excess in order to avoid hydrolysis and their exact HCl content was determined by titration with HCl 0.1 M (Titrisol) for values of pH $\geq$ 2. The titrant solution (0.1 M KOH) was prepared from a carbonate-free commercial concentrate (Titrisol) and standardized by titration with potassium hydrogen phthalate standard. This solution was rejected whenever the percentage of carbonate was higher than 0.5% of the total amount of the base.[42] Electronic spectra were recorded on a Perkin Elmer Lambda 35 spectrophotometer, using 1 cm path length thermostatic cells (25.0 ± 0.1 °C).

Synthesis of NTP(PrHPM)$_3$

The synthesis of the ligand starts with the preparation of the hydroxypyrimidinone side chains, involving the preliminary preparation of 1-(benzyloxy)-4-(1′,2′,4′-triazol-1′-yl)-2-(1*H*)-pyrimidinone[19] **1** and 3-((*tert*-butoxycarbonyl)amino)propylamine,[20] according to previously published procedures. Afterwards, those amine-bearing HPM arms are coupled to the tris-carboxylic backbone, nitrilotripropionic acid (NTP), *via* standard carboxyl activation methodologies. Final catalytic hydrogenolysis to remove the benzyl protecting groups affords the final NTP(PrHPM)$_3$ product.

4-[3-((*tert*-Butoxycarbonyl)amino)propylamino]-1-(benzyloxy)-2(1*H*)-pyrimidinone, 2. A solution of **1** (0.50 g, 1.86 mmol) and 3-((*tert*-butoxycarbonyl)amino)propylamine (0.39 g, 2.23 mmol) in dry THF (15 mL) was stirred for 16 h at reflux temperature, under a nitrogen atmosphere. The solvent was evaporated and H_2O added to the residue. The aqueous layer was extracted with $CHCl_3$ (5 × 20 mL) and the combined organic extracts were washed successively with 5% citric acid solution, H_2O, brine and dried over anhydrous magnesium sulfate. Evaporation of the solvent, followed by recrystallization of the residual solid from ethyl acetate, gave product **2** as a white amorphous solid (0.52 g, 74%). M.p. 162–164 °C; IR (KBr pellets): ν_{max}/cm^{-1} 3375, 3259, 3127, 3031, 1711, 1643, 1502, 1170. ^{1}H-NMR (400 MHz, $CDCl_3$): δ (ppm) 1.43 (9 H, s, OC-(CH_3)$_3$), 1.69 (2 H, q, J = 6.4 Hz, $CH_2CH_2CH_2$), 3.20 (2 H, t, J = 6.6 Hz, NHCH_2CH$_2$), 3.51 (2 H, t, J = 7.0 Hz, CH_2NHC(O)), 5.20 (2 H, s, PhCH_2), 5.35 (1 H, d, J = 6.0 Hz, NCH=C*H*C), 6.89 (1H, d, J = 9.0 Hz, NC*H*=CHC), 7.38 (5 H, s, Ph-*H*); ^{13}C-NMR (400 MHz, $CDCl_3$): δ (ppm) 28.4 (C(CH_3)$_3$), 29.7 ($CH_2CH_2CH_2$), 30.94 (CH_2NHC(O)), 37.0 (NHCH_2CH$_2$), 78.0 ($C_6H_5CH_2$), 79.6 (C(CH$_3$)$_3$), 93.6 (NCH=*C*HC), 128.7 (Ph-*C*2 and Ph-*C*6),

129.2 (Ph-*C*4), 130.1 (Ph-*C*3 and Ph-*C*5), 134.3 (Ph-*C*1), 142.5 (N*C*H=CHC), 153.2 (N*C*(O)N), 157.1 (NH*C*(O)-O), 162.4 (N=*C*NH).

4-(3-Aminopropylamino)-1-(benzyloxy)-2(1*H*)-pyrimidinone hydrochloride, 3. A solution of 4-[3-((*tert*-butoxycarbonyl)-amino)propylamino]-1-(benzyloxy)-2(1*H*)-pyrimidinone **2** (0.5 g, 1.33 mmol) in 4 M HCl 1,4-dioxane (8 mL) was stirred at 0 °C under a nitrogen atmosphere until complete consumption of **2** (4 h) as monitored by TLC. The reaction mixture was evaporated, dry ethanol was added to the residue, and then evaporated. This process was repeated 3 times to give product **3** as a white solid (0.4 g, 98%). M.p. 169–171 °C; IR (KBr pellets): ν_{max}/cm^{-1} 3447, 3033, 1735, 1654, 1275. ^{1}H-NMR (400 MHz, CD_3OD): δ (ppm) 2.06 (2 H, q, J = 8.0 Hz, $CH_2CH_2CH_2$), 3.08 (2 H, t, J = 8.0 Hz, $CH_2CH_2NH_2$), 3.54 (2 H, t, J = 8.0 Hz, $NHCH_2CH_2$), 5.24 (1.50 H, s, $C_6H_5CH_2$), 5.27 (0.50 H, s, $PhCH_2$), 5.98 (0.75 H, d, J = 8.0 H, NCH=CHC), 6.26 (0.25 H, d, J = 8.0 Hz, NCH=CHC), 7.44–7.54 (5 H, m, Ph-H), 7.88 (0.75 H, d, J = 8.0 Hz, NCH=CHC), 8.19 (0.25 H, d, J = 8.0 Hz, NCH=CHC); ^{13}C-NMR (400 MHz, CD_3OD): δ (ppm) 25.8 ($CH_2CH_2CH_2$), 36.6 ($NHCH_2CH_2$), 39.5 ($CH_2CH_2NH_2$), 79.2 ($C_6H_5CH_2$), 92.8 (NCH=CHC), 128.5 (Ph-C2 and Ph-C6), 129.3 (Ph-C4), 129.9 (Ph-C3 and Ph-C5), 133.0 (Ph-C1), 145.6 (NCH=CHC), 149.2 (NC(O)N), 158.3 (N=CNH).

3,3′,3″-Nitrilotri(*N*-(3-(1-(benzyloxy)-2-oxo-1,2-dihydropyrimidin-4-ylamino)propyl)-propanamide), 4. A mixture of 3,3′,3″-nitrilotripropanoic acid (NTP, 0.097 g, 0.414 mmol), TBTU (0.43 g, 1.37 mmol) and *N*-methylmorpholine (NMM, 0.30 mL, 2.73 mmol) in dry DMF (15 mL) containing molecular sieves was stirred at r.t. for 1 h. Meanwhile, a solution of **3** (0.450 g, 1.37 mmol) and NMM (0.30 mL, 2.73 mmol) in dry DMF (10 mL), also containing molecular sieves, was stirred at r.t. for 1 h. The first mixture was filtrated, the solution was added dropwise to the second one and the mixture was stirred under N_2 for 6 h. The final mixture was evaporated under vacuum. The crude material was taken into 0.1 M HCl (75 mL) and it was washed with CH_2Cl_2 (4 × 50 mL). Concentrated ammonia was added until a precipitate appeared (pH *ca.* 4), and it was extracted with CH_2Cl_2 (4 × 75 mL); the pH was raised again with ammonia (pH *ca.* 8–9), and the solution was extracted with more CH_2Cl_2 (3 × 75 mL). The total organic phase was dried over anhydrous Na_2SO_4, and then evaporated. The residue was washed with water (3 × 5 mL), and then with acetone. After recrystallization from MeOH/acetone, the final product was obtained, as a beige solid (0.153 g, 37% yield). M.p. 92–94 °C; MS (ESI+) m/z 1002.8 (100%) for $[M + H]^+$, 1024.8 (25%) for $[M + Na]^+$; ^{1}H-NMR (400 MHz, CD_3OD): δ (ppm) 1.57 (6 H, q, J = 6.8 Hz, $CONHCH_2CH_2CH_2$), 2.21 (6 H, t, J = 6.6 Hz, NCH_2CH_2CO), 2.61 (6 H, t, J = 6.6 Hz, NCH_2CH_2CO), 3.03 (6 H, q, J = 6.6 Hz, $CONHCH_2CH_2CH_2$), 3.19 (6 H, t, J = 6.8 Hz, $CONHCH_2CH_2CH_2$), 4.94 (6 H, s, $C_6H_5CH_2$), 5.41 (3 H, d, J = 7.6 Hz, NCH=CHC), 7.16 (3 H, d, J = 7.6 Hz, NCH=CHC), 7.19–7.26 (15 H, m, C_6H_5); ^{13}C-NMR (400 MHz, CD_3OD): δ (ppm) 29.8 ($CONHCH_2CH_2CH_2$), 34.7 (NCH_2CH_2CO), 37.8 ($CONHCH_2CH_2CH_2$), 39.3 ($CONHCH_2CH_2CH_2$), 50.7 (NCH_2CH_2CO), 79.5 ($C_6H_5CH_2$), 95.7 (NCH=CHC), 129.8 (Ph-*C*2 and Ph-*C*6), 130.4 (Ph-*C*4), 131.3 (Ph-*C*3 and Ph-*C*5), 135.3 (Ph-*C*1), 144.0 (NCH=CHC), 155.8 (NC(O)N), 164.4 (N=CNH), 175.0 (NCH_2CH_2CO).

3,3′,3″-Nitrilotri(*N*-(3-(1-hydroxy-2-oxo-1,2-dihydropyrimidin-4-ylamino)propyl)propanamide), NTP(PrHPM)$_3$. To a solution of **4** (0.090 g, 0.090 mmol) in MeOH (10 mL) was added 10% Pd/C (0.020 g), and the suspension was stirred under 2 bar H_2 atmosphere, at r.t. for 1 h. The solid was filtered off and the solution was evaporated. The residue was recrystallized from MeOH/acetone, affording the pure product as a white solid (0.060 g, 91% yield). M.p. 120–122 °C; MS (ESI+) m/z 732.5 (100%) for $[M + H]^+$, 754.5 (25%) for $[M + Na]^+$. Elemental analysis found, C, 49.33; H, 6.65; N, 24.63%; [$C_{30}H_{45}N_{13}O_9$·0.15 acetone] requires C, 49.39; H, 6.25; N, 24.59%; ^{1}H-NMR (400 MHz, D_2O, pD *ca.* 9, 1% MeOH): δ (ppm) 1.76 (6 H, q, J = 6.8 Hz, $CH_2CH_2CH_2$), 2.41 (6 H, t, J = 6.8 Hz, NCH_2CH_2CO), 2.78 (6 H, t, J = 7.0 Hz, NCH_2CH_2CO), 3.21–3.36 (12 H, m, $CH_2CH_2CH_2$), 5.74 (3 H, d, J = 7.2 Hz, NCH=CHC), 7.63 (3 H, d, J = 7.2 Hz, NCH=CHC); ^{13}C-NMR (400 MHz, D_2O, pD *ca.* 9, 1% MeOH): δ (ppm) 28.5 ($CONHCH_2CH_2CH_2$), 33.5 (NCH_2CH_2CO), 37.5 ($CONHCH_2CH_2CH_2$), 39.0 ($CONHCH_2CH_2CH_2$), 49.3.5 (NCH_2CH_2CO), 92.7 (NCH=CHC), 145.3 (NCH=CHC), 158.3 (NC(O)N), 161.4 (N=CNH), 175.5 (NCH_2CH_2CO).

Potentiometric studies

Measurements. Titrations of the ligands, alone and in the presence of aluminum (for NTP(PrHPM)$_3$) or of gallium (for HOPY-PrN), were performed in aqueous solution at T = 25.0 ± 0.1 °C and ionic strength (I) 0.1 M KCl.[43] For all the titrations involving NTP(PrHPM)$_3$, the total volume was 20 mL, the ligand concentration (C_L) was 4.0–5.0 × 10^{-4} M and C_{Al}/C_L was 0 : 1, 1 : 1.1 or 1 : 1.2. For the Ga^{3+}/HOPY-PrN system, the total volume was 20 mL, the ligand concentration was 1.0–2.0 × 10^{-3} M and C_{Ga}/C_L was 1 : 3. Each assay was done twice and the value determined for the ionization constant (pK_w) was 13.8.

Calculation of equilibrium constants. The stepwise protonation constants, $K_i = [H_iL]/[H_{i-1}L][H]$ (i = 1–7), and the overall metal-complex stability constants, $\beta_{M_mH_hL_l} = [M_mH_hL_l]/[M]^m[H]^h[L]^l$, were determined by fitting analysis of the potentiometric data with the HYPERQUAD 2008 program.[27] Al^{3+} and Ga^{3+} hydroxide species[40–42] were included in the equilibrium complexation model and the species distribution curves were obtained with the HYSS program.[27]

Spectroscopic studies

Measurements. ^{1}H NMR titration of NTP(PrHPM)$_3$ (5 × 10^{-4} M in D_2O) was performed as previously described,[23] and the final pD values were determined from the equation pD = pH* + 0.4,[26] in which pH* corresponds to the reading of the pH meter previously calibrated with aqueous buffers at pH 4 and 7. The electronic spectra of HOPY-PrN (C_L = 1.9 × 10^{-4} M) were recorded in the range 200–400 nm and those for the 1 : 1 Ga^{3+}/HOPY-PrN system were obtained in the range 250–380 nm

(C_L = 1.9 × 10^{-4} M, 1 : 1 stoichiometry). For NTP(PrHPM)$_3$ (C_L = 5.0 × 10^{-5} M) the electronic spectra were recorded in the range 200–400 nm, while those of the corresponding Fe^{3+} and Ga^{3+} complexes were collected in the range 300–700 nm (C_L = 2.7 × 10^{-4} M) and 200–400 nm (C_L = 5.0 × 10^{-5} M), respectively, under a 1 : 1.2 stoichiometry. For pH ≥ 2, solutions of complexes were prepared as indicated for the potentiometric measurements. Both Fe^{3+}–NTP(PrHPM)$_3$ and Ga^{3+}–NTP(PrHPM)$_3$ systems were studied for pH below 2 (0.8–2), using a batch titration (7 points), in which the amount of acid added (from standard 0.1 or 1 M HCl solutions) was calculated for the total volume solution used.

Calculation of equilibrium constants. The overall iron and gallium complex stability constants of NTP(PrHPM)$_3$, as well as the value of β_{GaHL} for HOPY-PrN, were determined with the PSEQUAD program,[28] by fitting analysis of the spectrophotometric data and including in the equilibrium model the data for Fe^{3+} and Ga^{3+} hydrolytic species.[44–46]

Determination of partition coefficients

The octanol–water partition coefficients (log *P*) of NTP(PrHPM)$_3$ and HOPY-PrN were determined by the "shakeflask" method,[47,48] which is based on the concentration ratio of the compounds between 1-octanol and a TRIS buffered aqueous phase (pH = 7.4). The species concentrations were assessed by spectrophotometry, based on the absorbance of the benzenoid bands (π–π*) of the compounds.

Molecular modeling

The structure of the Fe^{3+}–NTP(PrHPM)$_3$ complex was optimized by quantum mechanical calculations based on Density Functional Theory (DFT) methods, using the Gaussian-03W software.[37] This energy minimization was carried out using the functional B3LYP chemical model, and it was performed in two steps. In the first step the 3-21G basis set was used with a direct self-consistent field method (SCF) and SCF convergence criterion of 10^{-5}. The results of these calculations were subjected to a deeper second optimization step using the LANL2DZ basis with the same SCF settings. The functional B3LYP has been shown to be an accurate density functional method,[49] and it has proved to give reliable geometries and energies for complexes with several metal ions, namely transition metal ions.[50] The B3LYP model is a combination of the Becke three-parameter hybrid functional[51] with the Lee–Yang–Parr correlation functional (which also includes density gradient terms).[52,53] Regarding the basis set, 3-21G is the simplest of Pople's split-valence basis sets, and it can be used with relatively good accuracy for molecules containing first and second-row elements.[54] It has been used in our first calculation step, mostly in order to optimize the conformation of the ligand. The LANL2DZ basis set specifies the Dunning–Huzinaga valence double-zeta basis set (D95V) on the first row (all the atoms of the ligand),[55] and Los Alamos ECP plus DZ on Na–Bi.[56] In this way, the Fe atom is described through the Los Alamos ECP and a double-zeta basis set including 3d orbitals and 3d diffuse functions for the valence shell.

Biodistribution studies

In vivo biodistribution studies were carried out in groups of 3–5 female CD1 mice (randomly bred, Charles River, from CRIFFA, Barcelona, Spain) weighing *ca.* 25 g, ^{67}Ga-citrate injection solution was prepared by dilution of ^{67}Ga citrate from MDS Nordion (Ottawa, Canada) with saline to obtain a final radioactive concentration of 5–10 MBq per 100 μL. The ^{67}Ga–NTP(PrHPM)$_3$ complex was synthesized by adding ^{67}Ga-citrate to a saline solution of NTP(PrHPM)$_3$ and the radiochemical purity, superior to 95%, was determined by ITLC, as reported before. Mice were intravenously (i.v.) injected with 100 μL (5–10 MBq) of ^{67}Ga citrate *via* the tail vein. In a separate group of animals the i.v. administration was immediately followed by intraperitoneal (i.p.) injection of 0.5 μmol of the ligand in 100 μL saline solution. Biodistribution of the ^{67}Ga–NTP(PrHPM)$_3$ complex was assessed by i.v. injection of 100 μL of the complex solution previously prepared. Animals were maintained on normal diet *ad libitum* and were sacrificed by cervical dislocation at 15 min, 1 h, 4 h and 24 h post-administration. The administered radioactive dose and the radioactivity in sacrificed animals were measured in a dose calibrator (Aloka, Curiemeter IGC-3, Tokyo, Japan). The difference between the radioactivity in the injected and sacrificed animal was assumed to be due to whole body excretion. Tissue samples of main organs were then removed for counting in a gamma counter (Berthold LB2111, Berthold Technologies, Germany). Biodistribution results were expressed as percent of injected activity per total organ (%I.A./organ) and presented as mean values ±SD. For blood, bone and muscle, total activity was calculated assuming, as previously reported, that these organs constitute 7, 10 and 40% of the total weight, respectively.

Acknowledgements

The authors thank the Portuguese NMR Network (IST-UTL Center) for providing access to the NMR facilities, the Portuguese *Fundação para a Ciência e Tecnologia* (FCT) (project PTDC/QUI/65647/2006 and post-Doc grant SFRH/BPD/29874/2006 – S. M.) as well as PEst-OE/QUI/UI0100/2011 for financial support.

References

1 R. R. Crichton, in *Inorganic Biochemistry of Iron Metabolism: From Molecular Mechanisms to Clinical Consequences*, Wiley, Chichester, 2001.
2 G. Faa and G. Crisponi, *Coord. Chem. Rev.*, 1999, **184**, 291–310.
3 R. A. Yokel and P. J. McNamara, *Pharmacol. Toxicol.*, 2001, **88**, 159–167.

4 G. Crisponi, V. M. Nurchi, G. Faa and M. Remelli, *Monatsh. Chem.*, 2011, **142**, 331–340.
5 P. Zatta, *J. Alzheimers Dis.*, 2006, **10**, 33–37.
6 C. Exley, *J. Inorg. Biochem.*, 1999, **76**, 133–140.
7 L. E. Scott and C. Orvig, *Chem. Rev.*, 2009, **109**, 4885.
8 G. Crisponi, V. M. Nurchi, V. Bertolasi, M. Remelli and G. Faa, *Coord. Chem. Rev.*, 2012, **256**, 89–104.
9 M. A. Santos, M. A. Esteves and S. Chaves, *Curr. Med. Chem.*, 2012, **19**, 2773–2793.
10 W. R. Harris and J. Sheldon, *Inorg. Chem.*, 1990, **29**, 119–124.
11 R. D. Propper, S. B. Shurin and D. G. Nathan, *N. Engl. J. Med.*, 1976, **294**, 1421–1423.
12 R. C. Hider, G. Kontoghiorghes, J. Silver and M. A. Stockham, *UK Pat.*, 2117766, 1982.
13 U. Heinz, K. Hegetschweiber, P. Acklin, B. Faller, R. Lattmann and H. P. Schnebli, *Angew. Chem., Int. Ed.*, 1999, **38**, 2568–2570.
14 R. A. Yokel, P. Ackrill, E. Burgess, J. P. Day, J. L. Domingo, T. P. Flaten and J. Savory, *J. Toxicol. Environ. Health*, 1996, **48**, 667–683.
15 Z. D. Liu and R. C. Hider, *Med. Res. Rev.*, 2002, **22**, 26–64.
16 M. A. Santos, S. M. Marques and S. Chaves, *Coord. Chem. Rev.*, 2012, **256**, 240–259.
17 M. A. Santos, *Coord. Chem. Rev.*, 2008, **252**, 1213–1224.
18 S. Chaves, S. Marques, A. M. F. Matos, A. Nunes, L. Gano, T. Tuccinardo, A. Martinelli and M. A. Santos, *Chem.–Eur. J.*, 2010, **16**, 10535–10545.
19 M. A. Esteves, A. Cachudo, S. Chaves and M. A. Santos, *Eur. J. Inorg. Chem.*, 2005, 597–605.
20 D. Boturyn, A. Boudali, J. F. Constant, E. Defrancq and J. Lhomme, *Tetrahedron*, 1997, **53**, 5485–5492.
21 A. Katoh, Y. Hida, J. Kamitani and J. Ohkanda, *J. Chem. Soc., Dalton Trans.*, 1998, 3859–3864.
22 S. Chaves, A. C. Mendonça, S. M. Marques, M. I. M. Prata, A. C. Santos, A. F. Martins, C. F. G. C. Geraldes and M. A. Santos, *J. Inorg. Biochem.*, 2011, **105**, 31–38.
23 M. A. Santos, M. Gil, S. Marques, L. Gano, G. Cantinho and S. Chaves, *J. Inorg. Biochem.*, 2002, **92**, 43–54.
24 E. T. Clarke and A. E. Martell, *Inorg. Chim. Acta*, 1992, **196**, 185–194.
25 R. A. Yokel, A. K. Datta and E. G. Jackson, *J. Pharmacol. Exp.Ther.*, 1991, **257**, 100–106.
26 A. K. Covington, M. Paabo, R. A. Robinson and R. G. Bates, *Anal. Chem.*, 1968, **40**, 700–706.
27 A. Gans, A. Sabatini and A. Vacca, *Talanta*, 1996, **43**, 1739–1753.
28 L. Zékány, I. Nagypál and G. Peintler, *PSEQUAD version 5.01*, 2001.
29 J. Okhanda, J. Kamitani, T. Tokumitsu, Y. Hida, T. Konakahara and A. Katoh, *J. Org. Chem.*, 1997, **62**, 3618–3624.
30 M. A. Santos, S. Gama, L. Gano, G. Cantinho and E. Farkas, *Dalton Trans.*, 2004, 3772–3781.
31 S. Gama, P. Dron, S. Chaves, E. Farkas and M. A. Santos, *Dalton Trans.*, 2009, 6141–6150.
32 A. E. Martell, R. M. Smith and R. J. Motekaitis, in *Critically Selected Stability Constants of Metal Complexes Database*, College Station TX, version 4, 1997.
33 R. J. Motekaitis and A. E. Martell, *Inorg. Chim. Acta*, 1991, **183**, 71–80.
34 A. Evers, R. D. Hancock, A. E. Martell and R. J. Motekaitis, *Inorg. Chem.*, 1989, **28**, 2189–2195.
35 W. R. Harris and V. L. Pecoraro, *Biochemistry*, 1983, **22**, 292–299.
36 J. Beardmore and C. Exley, *J. Inorg. Biochem.*, 2009, **103**, 205–209.
37 M. J. Frisch, G. W. Trucks, H. B. Schlegel, G. E. Scuseria, M. A. Robb, J. R. Cheeseman, J. A. Montgomery, Jr., T. Vreven, K. N. Kudin, J. C. Burant, J. M. Millam, S. S. Iyengar, J. Tomasi, V. Barone, B. Mennucci, M. Cossi, G. Scalmani, N. Rega, G. A. Petersson, H. Nakatsuji, M. Hada, M. Ehara, K. Toyota, R. Fukuda, J. Hasegawa, M. Ishida, T. Nakajima, Y. Honda, O. Kitao, H. Nakai, M. Klene, X. Li, J. E. Knox, H. P. Hratchian, J. B. Cross, V. Bakken, C. Adamo, J. Jaramillo, R. Gomperts, R. E. Stratmann, O. Yazyev, A. J. Austin, R. Cammi, C. Pomelli, J. W. Ochterski, P. Y. Ayala, K. Morokuma, G. A. Voth, P. Salvador, J. J. Dannenberg, V. G. Zakrzewski, S. Dapprich, A. D. Daniels, M. C. Strain, O. Farkas, D. K. Malick, A. D. Rabuck, K. Raghavachari, J. B. Foresman, J. V. Ortiz, Q. Cui, A. G. Baboul, S. Clifford, J. Cioslowski, B. B. Stefanov, G. Liu, A. Liashenko, P. Piskorz, I. Komaromi, R. L. Martin, D. J. Fox, T. Keith, M. A. Al-Laham, C. Y. Peng, A. Nanayakkara, M. Challacombe, P. M. W. Gill, B. Johnson, W. Chen, M. W. Wong, C. Gonzalez and J. A. Pople, *GAUSSIAN 03 (Revision C.02)*, Gaussian, Inc., Wallingford CT, 2004.
38 C. B. Dobson, J. P. Day, S. J. King and R. F. Itzhaki, *Toxicol. Appl. Pharmacol.*, 1998, **152**, 145–152.
39 A. Radunovic, H. T. Delves and M. W. B. Bradbury, *Biol. Trace Elem. Res.*, 1998, **62**, 51–64.
40 R. C. Walton, K. N. White, F. Livens and C. R. McCrohan, *Biometals*, 2010, **23**, 221–230.
41 W. L. F. Armarego and D. D. Perrin, in *Purification of Laboratory Chemicals*, Butterworth-Heinemann Press, Oxford, 4th edn, 1999.
42 F. J. C. Rossotti and H. Rossotti, *J. Chem. Ed.*, 1965, **42**, 375–378.
43 S. Chaves, M. Gil, S. Marques, L. Gano and M. A. Santos, *J. Inorg. Biochem.*, 2003, **97**, 161–172.
44 C. F. Baes and R. E. Mesmer, in *The Hydrolysis of Cations*, Wiley, New York, 1st edn, 1976.
45 L. O. Öhman and W. Forschling, *Acta Chim. Scand. Ser. A*, 1981, **35**, 795–802.
46 R. M. Smith and A. E. Martell, in *Critical Stability Constants*, Plenum Press, New York, 1st edn, 1976, vol. 4, p. 11.
47 M. A. Santos, M. Gil, L. Gano and S. Chaves, *J. Biol. Inorg. Chem.*, 2005, **10**, 564–580.
48 A. Leo, C. Hansch and D. Elkins, *Chem. Rev.*, 1971, **71**, 526–616.
49 C. W. Bauschlicher, *Chem. Phys. Lett.*, 1995, **246**, 40–44.

50 A. Ricca and C. W. Bauschlicher, *Theor. Chim. Acta*, 1995, **92**, 123–131.
51 D. Becke, *Phys. Rev. A*, 1988, **38**, 3098–3100.
52 C. Lee, W. Yang and R. G. Parr, *Phys. Rev. B: Condens. Matter*, 1988, **37**, 785–789.
53 B. Miehlich, A. Savin, H. Stoll and H. Preuss, *Chem. Phys. Lett.*, 1989, **157**, 200–206.
54 M. S. Gordon, J. S. Binkley, J. A. Pople, W. J. Pietro and W. J. Hehre, *J. Am. Chem. Soc.*, 1982, **104**, 2797–2803.
55 T. H. Dunning Jr. and P. J. Hay, in *Modern Theoretical Chemistry*, ed. H. F. Schaefer, III, Plenum, New York, 1976, vol. 3, pp. 1–28.
56 P. J. Hay and W. R. Wadt, *J. Chem. Phys.*, 1985, **82**, 299–310.